JMEPEG (2016) 25:5209–5219
DOI: 10.1007/s11665-016-2384-x

1059-9495/$19.00

The Tribological Performance of Surface Treated Ti6A14V as Sliding Against Si_3N_4 Ball and 316L Stainless Steel Cylinder

W.H. Kao, Y.L. Su, J.H. Horng, and H.C. Huang

(Submitted April 5, 2016; in revised form September 27, 2016; published online October 11, 2016)

Closed field unbalanced magnetron sputtering was used to deposit diamond-like carbon (Ti-C:H) coatings on Ti6Al4V alloy and gas nitrided Ti6Al4V alloy. Four different specimens were prepared, namely untreated Ti6Al4V alloy (Ti6Al4V), gas nitrided Ti6Al4V alloy (N-Ti6Al4V), Ti-C:H-coated Ti6Al4V alloy (Ti-C:H/Ti6Al4V) and Ti-C:H-coated gas nitrided Ti6Al4V alloy (Ti-C:H/N-Ti6Al4V). The tribological properties of the four specimens were evaluated using a reciprocating wear tester sliding against a Si_3N_4 ball (point contact mode) and 316L stainless steel cylinder (line contact mode). The wear tests were performed in a 0.89 wt.% NaCl solution. The results showed that the nitriding treatment increased the surface roughness and hardness of the Ti6Al4V alloy and improved the wear resistance as a result. In addition, the Ti-C:H coating also improved the tribological performance of Ti6Al4V. For example, compared to the untreated Ti6Al4V sample, the Ti-C:H coating reduced the wear depth and friction coefficient by 340 times and 10 times, respectively, in the point contact wear mode, and 151 times and 9 times, respectively, in the line contact wear mode. It is thus inferred that diamond-like carbon coatings are of significant benefit in extending the service life of artificial biomedical implants.

Keywords nitrided Ti6Al4V alloy, Ti-C:H coating, tribological properties

1. Introduction

Surgical implants are generally made from ultra-high molecular weight polyethylene. However, while such implants have a low weight, they also have a low strength and are thus prone to wear following prolonged use. The particulate wear debris stimulate mononuclear cells to secrete cytokines, activate osteoclast for bone resorption, prompt osteolysis and cause an eventual loosening of the implant (Ref 1, 2). To resolve these problems, several researchers have suggested replacing polyethylene with ceramic or metal materials with a higher wear resistance (Ref 3, 4). However, ceramic materials in particular tend to crack under shock and are therefore unsuitable for young patients (below 50 years of age) or those who perform regular strenuous exercise (Ref 5, 6). Mainstream metal implant materials mainly comprise stainless steel, titanium alloy and chrome alloy; all of which have excellent passivity (and thus good biological compatibility) due to their ready oxidation in air and a high corrosion resistance (Ref 7). Moreover, their elastic coefficients are approximately the same as that of bone, and their strength is higher than that of high molecular weight materials. However, they have a poorer wear resistance than ceramic materials. For example, the service life of an artificial all-metal hip joint for patients above 65 years old is around 15 years (Ref 8), whereas that of an artificial all-ceramic hip joint is over 20 years (Ref 9).

Diamond-like carbon (DLC) films have high hardness, high wear resistance, low friction, high chemical passivity and good biological compatibility. Consequently, DLC films have significant potential for the surface protection of medical implants. Various studies have demonstrated the effectiveness of DLC coatings in preventing the proliferation of bacteria on stainless steel or silicon substrates (Ref 10-13). Furthermore, DLC coatings on biomedical stainless steel (Ref 14) and NiTi alloy (Ref 15) provide good wear resistance when sliding against high density polyethylene and Si_3N_4, respectively. Importantly, DLC coatings also have good biocompatibility. For example, many studies have shown that DLC coatings on silicon wafers (Ref 16, 17), Si_3N_4 ceramic materials (Ref 18) and polycarbonate tissue culture inserts (Ref 19) promote the proliferation of cells. Moreover, due to their excellent hemocompatibility, DLC coatings can also be applied to cardiovascular implants, such as artificial heart valves and stents, blood pumps (Ref 20).

Once human implants are implanted, it is not only extremely expensive to remove or replace them, but also causes the patient further suffering and pain. Consequently, it is essential to maximize the service life of biomedical implants through an appropriate choice of implant material or surface treatment. Previous studies have shown that DLC films coated on Ti6Al4V alloy substrates previously treated by N_2 plasma (Ref 21), O_2 plasma (Ref 22), or micro-arc oxidation (Ref 23) yield a significant improvement in the wear resistance. Accordingly, this study investigates the mechanical properties, metallographic structures and tribological performance of four Ti6Al4V samples, namely untreated Ti6Al4V alloy (Ti6Al4V), gas nitrided Ti6Al4V alloy (N-Ti6Al4V), Ti-C:H-coated Ti6Al4V alloy (Ti-C:H/Ti6Al4V) and Ti-C:H-coated gas

W.H. Kao and **H.C. Huang**, Institute of Mechatronoptic Systems, Chienkuo Technology University, Changhua, Taiwan; **Y.L. Su**, Department of Mechanical Engineering, National Cheng Kung University, Tainan, Taiwan; and **J.H. Horng**, Department of Power Mechanical Engineering, National Formosa University, Yunlin, Taiwan. Contact e-mail: n18851158@yahoo.com.tw.

nitrided Ti6Al4V alloy (Ti-C:H/N-Ti6Al4V). Overall, the results provide a useful insight into the optimal surface treatment for Ti6Al4V biomedical implants.

2. Experimental Method

2.1 High-Temperature Gas Nitridation

Previous studies have shown that the wear resistance of nitrided Ti6Al4V alloy increases with an increasing temperature and plasma nitriding time under vacuum conditions. For example, the authors in Ref 24 enhanced the wear resistance of Ti6Al4V alloy by performing the nitriding process at a temperature of 750 °C using a processing time of 4 h and a pressure of 2.5 Pa. Similarly, the authors in Ref 25 performed nitriding using a temperature of 900 °C, a processing time of 12 h and a pressure of 0.0013 Pa. In the present study, Ti6Al4V samples with an average surface roughness of Ra = 0.021 μm were nitrided in a pure nitrogen environment. The nitriding process was performed at temperatures of 600, 800, 860 and 900 °C for soaking times of 30, 30, 10 and 120 min, respectively. The heating rate was set as 10 °C/min in every case. Following the nitriding process, the samples were cooled to 60 °C at a rate of 84 °C/min, removed and then placed in an atmospheric environment. Having cooled to room temperature, the samples were polished with 0.05 μm Al_2O_3 to remove any loose structures or surface impurities. The final surface roughness was found to be Ra = 0.127 μm.

2.2 Diamond-Like Carbon Coating Deposition

According to a previous study by the present group (Ref 26), diamond-like (Ti-C:H) coatings with a 3.5 at.% titanium content exhibit excellent tribological properties. Therefore, the titanium content in the present Ti-C:H coatings was also controlled to approximately 3.5 at.%. The Ti-C:H coatings were deposited on nitrided and non-nitrided Ti6Al4V substrates using a closed field unbalanced magnetron sputtering system. The sputtering process was performed using a DC frequency of 50 kHz, a chamber pressure of 0.4 Pa, three graphite targets and a single titanium target. In addition, the table rotation speed was set as 3 rpm, methane was used as the reactive gas and Ar plasma was used as the sputtering source (flow rate: 30 sccm). The sputtering process commenced by depositing a 0.1-μm pure Ti transition layer on the substrate using a Ti target current of 1 A and a substrate voltage bias of −42 V for 20 min. A hydrogenous Ti-C:H topcoat was then deposited on the Ti transition layer using a Ti target current of 0.4 A, graphite target currents of 2.3 A, a substrate voltage bias of −42 V and a methane flow rate of 3 sccm for 100 min.

2.3 Surface Morphology, Roughness, Hardness, Adhesion Analysis and Chemical Composition

To observe the nitrided layer, 5% hydrofluoric acid solution was evenly spread on the surface of the nitrided N-Ti6Al4V specimens for around 5 s. The nitrided layer was then examined using optical microscopy (OM). In addition, the Ti-C:H coatings on the various specimens were observed using field emission scanning electron microscopy (FE-SEM). The hardness of the Ti-C:H-coated samples (Ti-C:H/Ti6Al4V and Ti-C:H/N-Ti6Al4V) was evaluated using an LBI Nanoindenter (UNAT-M, Germany) with a Berkovich diamond tip and a maximum applied load of 5 mN. The hardness of the uncoated samples was measured using a Knoop hardness tester under a constant load of 10 g for 15 s. For all of the samples, the hardness was taken as the average value obtained over eight separate measurements. The adhesion properties of the Ti-C:H coatings were evaluated in accordance with the failure mode observed in indentation tests (Ref 27) performed using a Rockwell hardness machine under a load of 150 kgf. Finally, the chemical compositions of the sample surfaces were evaluated via energy-dispersive x-ray spectroscopy (EDS).

2.4 Tribological Properties

The tribological properties of the various samples were evaluated using a reciprocating wear tester in both the point contact mode and the line contact mode. The point contact wear tests were performed using a Si_3N_4 ceramic ball with a diameter of 10 mm, while the line contact wear tests were performed using a 316L stainless steel cylinder with a length and diameter of 22 and 15 mm, respectively. In the point contact wear tests, the load was set as 10, 20 and 30 N. The line contact wear tests were performed under loads of 100, 150 and 200 N, respectively. For both wear modes, the stroke length was set as 1 mm,

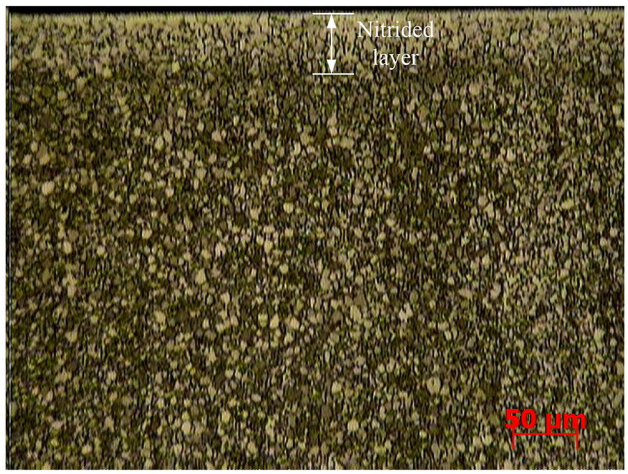

(a)

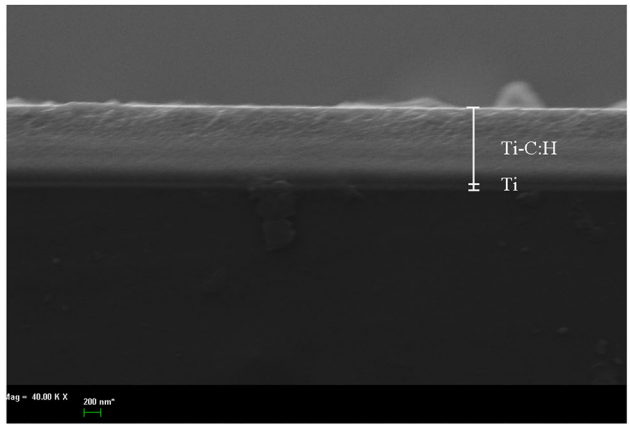

(b)

Fig. 1 (a) Sectional metallographic image of N-Ti6Al4V nitrided layer and (b) sectional metallographic image of Ti-C:H coating on Ti6Al4V substrate

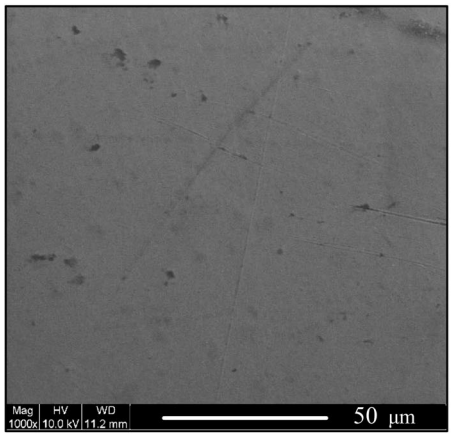

Element	Al	Ti	V
At%	12.71	83.78	03.51

(a)

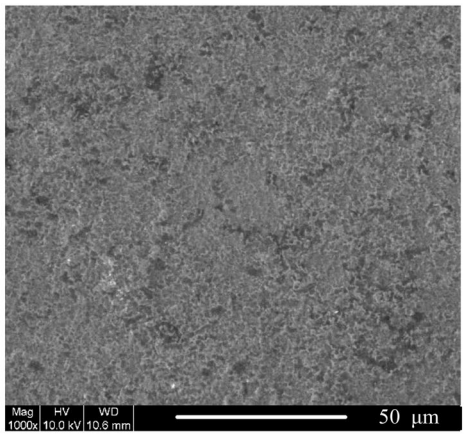

Element	N	Al	Ti	V
At%	22.87	3.13	73.68	0.32

(b)

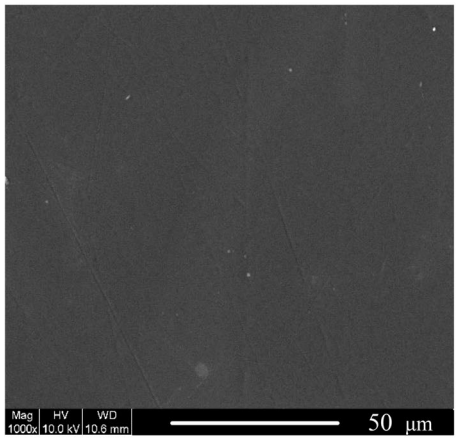

Element	C	Ti
At%	97.10	02.90

(c)

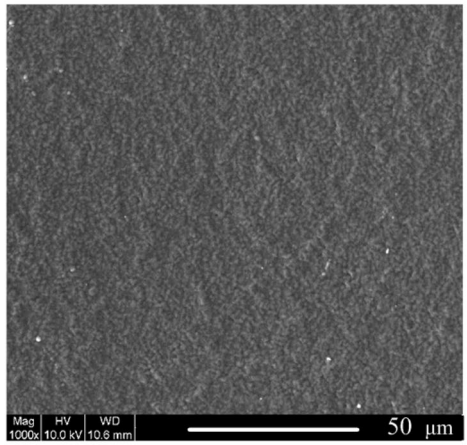

Element	C	Ti
At%	96.61	03.39

(d)

Fig. 2 SEM micrographs and chemical compositions of: (a) Ti6Al4V, (b) N-Ti6Al4V, (c) Ti-C:H/Ti6Al4V and (d) Ti-C:H/N-Ti6Al4V samples

the sliding frequency as 50 Hz and the total test time as 24 min. Furthermore, all of the tests were performed in a 0.89 wt.% NaCl solution. After the experiments, the friction coefficient, wear width and wear depth were recorded for all of the specimens. Moreover, the wear surfaces were examined by FE-SEM and EDS.

3. Results and Discussion

3.1 Surface Morphology, Roughness, Hardness, Adhesion Analysis and Chemical Composition

Figure 1(a) shows an OM image of the gas nitrided layer on the surface of the N-Ti6Al4V sample. It is seen that the nitrided layer has a depth of approximately 50 µm. The chemical composition of the nitrided layer was evaluated using a glow discharge spectrometer (LECO GDS-750 QDP, America) operated with a DC power source (600-1500 V). The relative concentration (at.%) of N was found to reduce from around 26% at the surface to approximately 9% at a depth of 1.2 µm and 1.3% at a depth of 10 µm. In addition, the Ti, V and Al concentrations at a depth of 10 µm were around 83, 3.2 and 12.5%, respectively, and approached those of the untreated sample (i.e., 83.78, 3.51 and 12.71%) at a depth of around 50 µm. Figure 1(b) presents a cross-sectional SEM image of the Ti-C:H/Ti6Al4V sample. As shown, the DLC coating has a non-columnar crystal structure and a thickness of around 1 µm.

As shown in Fig. 2(a), the untreated Ti6Al4V sample has a smooth surface with a roughness of approximately Ra = 0.021 µm and a hardness of 3.16 GPa. For the N-Ti6Al4V sample, the surface contains a large number of wrinkles. Moreover, the surface roughness and hardness increase to Ra = 0.127 µm and 9.05 GPa, respectively. For the Ti-C:H/Ti6Al4V and Ti-C:H/N-Ti6Al4V samples, the surface roughness is Ra = 0.03 µm and Ra = 0.175 µm, respectively (see Fig. 2c and d). Figure 2 also shows the EDS analysis results for the surface compositions of the

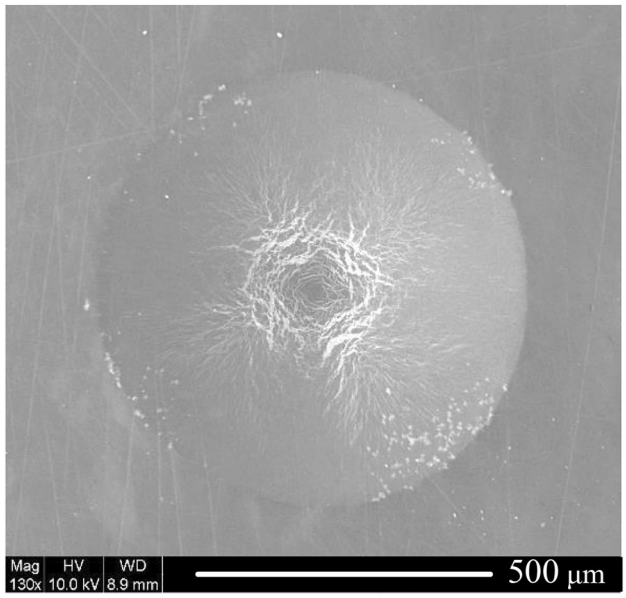

(a)

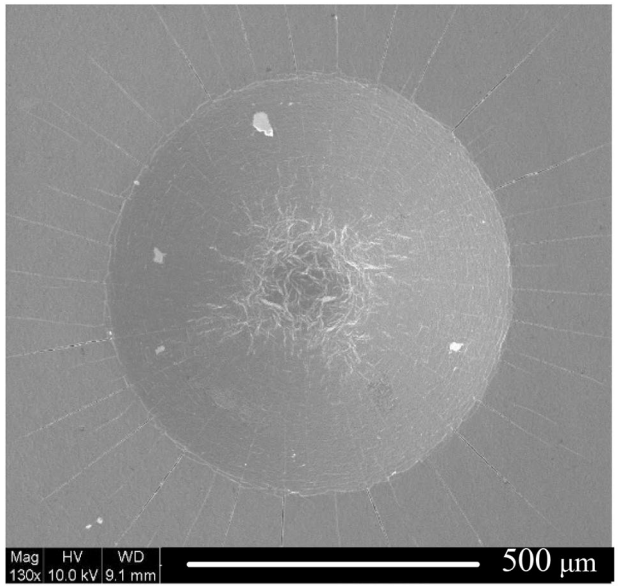

(b)

Fig. 3 Rockwell indentation results for: (a) Ti-C:H/Ti6Al4V and (b) Ti-C:H/N-Ti6Al4V samples

samples. It is seen that the Ti6Al4V sample contains 12.71% Al, 83.78% Ti and 3.51% V (Fig. 2a), while the N-Ti6Al4V sample consists of 22.87% N, 3.13% Al, 73.68% Ti and 0.32% V (Fig. 2b). For the coated samples, the Ti-C:H/Ti6Al4V specimen consists of 97.10% C and 2.90% Ti (Fig. 2c), while the Ti-C:H/N-Ti6Al4V sample contains 96.61% C and 3.39% Ti (Fig. 2d). The Ti-C:H/Ti6Al4V and Ti-C:H/N-Ti6Al4V coatings were found to have hardness values of 16.71 and 16.90 GPa, respectively. In a previous study (Ref 28), it was shown that the coating hardness is unaffected by the underlying substrate if the maximum indentation depth is less than one-tenth of the coating thickness. In the present study, the maximum indentation depths of the Ti-C:H/Ti6Al4V and Ti-C:H/N-Ti6Al4V samples were 73±6 and 71±4 nm, respectively. Therefore, the indentation depth was less than one-tenth of the Ti-C:H coating thickness (1000 nm) for both samples, and hence, the substrate effect can be ignored. Figure 3(a) presents an SEM image of the indented Ti-C:H/Ti6Al4V sample. It is seen that the region of the coating around the indentation contains almost no cracks. In other words, the coating has excellent adhesion properties [i.e., Class A (Ref 27)]. Figure 3(b) shows that the coating around the indentation in the Ti-C:H/N-Ti6Al4V sample contains a small number of cracks. However, the coating is still judged to have Class A adhesion properties.

3.2 Tribological Properties

3.2.1 Friction and Wear Resistance Properties in Point Contact Mode. Figure 4(a) shows the average friction coefficients of the Ti6Al4V, N-Ti6Al4V, Ti-C:H/Ti6Al4V and Ti-C:H/N-Ti6Al4V samples when sliding against the Si_3N_4 ball under loads of 10, 20 and 30 N, respectively. It is seen that for all four samples, the friction coefficient reduces slightly with an increasing load. The Ti6Al4V and N-Ti6Al4V specimens both have high friction coefficients in the range of 0.5∼0.7. However, the coated Ti-C:H/Ti6Al4V and Ti-C:H/N-Ti6Al4V samples have friction coefficients ranging from 0.042 to 0.079, i.e., around 10 times lower than those of the uncoated samples. Figure 4(b) shows the friction coefficient trajectories of the four samples in the point contact wear mode tests performed under a load of 10 N. The untreated Ti6Al4V sample has an average friction coefficient of around 0.704, while the nitrided N-Ti6Al4V sample has an average friction coefficient of approximately 0.706. In both cases, the friction coefficient fluctuates severely over the course of the wear test. The average friction coefficients of the Ti-C:H/Ti6Al4V and Ti-C:H/N-Ti6Al4V samples are 0.065 and 0.079, respectively, i.e., significantly lower than those of their uncoated counterparts. Moreover, the trajectories remain smooth and stable over the entire test duration. In other words, the Ti-C:H coating provides an effective reduction in the friction force acting at the sliding contact surface.

Figure 5(a) shows the average wear depths of the Ti6Al4V, N-Ti6Al4V, Ti-C:H/Ti6Al4V and Ti-C:H/N-Ti6Al4V samples in the point contact wear tests performed under loads of 10, 20 and 30 N. For all four samples, the wear depth increases with an increasing load. The untreated Ti6Al4V sample has average wear depths of 20.4, 27.1 and 32.8 µm under the considered loads. However, following nitriding, the corresponding wear depths reduce to 5.13, 8.11 and 15.1 µm, respectively. The Ti-C:H-coated specimens have extremely low wear depths, i.e., 0.06, 0.29 and 0.4 µm (Ti-C:H/Ti6Al4V) and 0.14, 0.47 and 0.57 µm (Ti-C:H/N-Ti6Al4V), respectively. From inspection, the wear depths of the Ti-C:H/Ti6Al4V sample under loads of 10, 20 and 30 N are around 340, 93 and 82 times lower than those of the untreated Ti6Al4V sample, respectively. In other words, the Ti-C:H coating provides an excellent anti-wear performance. Figure 5(b) shows the wear profiles of the four samples following the point contact wear tests performed under a load of 10 N. It is observed that the untreated Ti6Al4V sample experiences the greatest wear, with an average wear depth and width of 20.4 and 820 µm, respectively. For the N-Ti6Al4V sample, the wear depth and wear width reduce to 5.13 and 460 µm, respectively. In other words, the nitriding treatment increases the hardness of the Ti6Al4V alloy and therefore improves its resistance to plastic deformation and reduces its wear depth. The wear profiles of the Ti-C:H/

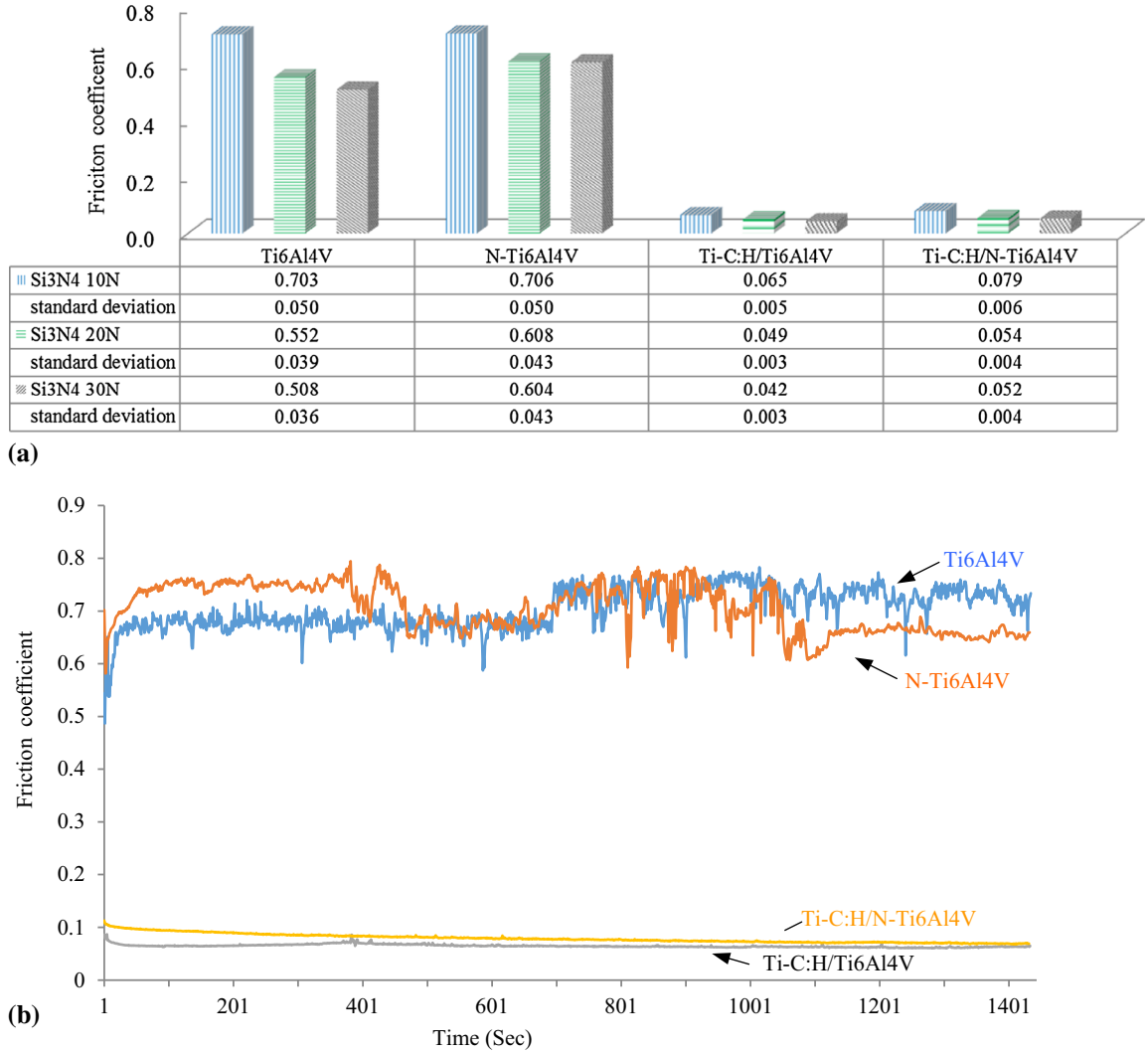

	Ti6Al4V	N-Ti6Al4V	Ti-C:H/Ti6Al4V	Ti-C:H/N-Ti6Al4V
Si3N4 10N	0.703	0.706	0.065	0.079
standard deviation	0.050	0.050	0.005	0.006
Si3N4 20N	0.552	0.608	0.049	0.054
standard deviation	0.039	0.043	0.003	0.004
Si3N4 30N	0.508	0.604	0.042	0.052
standard deviation	0.036	0.043	0.003	0.004

Fig. 4 Ti6Al4V samples sliding against Si_3N_4 ball: (a) histograms of average friction coefficient under loads of 10, 20 and 30 N and (b) friction coefficient trajectories under sliding load of 10 N

Ti6Al4V and Ti-C:H/N-Ti6Al4V samples are almost indistinguishable in Fig. 5(b). Hence, a magnified view of the two profiles is shown in Fig. 5(c). It is seen that the Ti-C:H/Ti6Al4V sample has a wear depth and wear width of 0.06 and 80 μm, respectively, while the Ti-C:H/N-Ti6Al4V sample has a wear depth of 0.14 μm and a wear width of 120 μm. In other words, the Ti-C:H coating reduces the wear depth of the Ti6Al4V sample by around 340 times. The surface roughness of the Ti-C:H/N-Ti6Al4V sample is around Ra = 0.175 μm, i.e., approximately 5.8 times higher than that of the Ti-C:H/Ti6Al4V sample (Ra = 0.03 μm). The higher surface roughness increases the friction coefficient, and hence, the wear depth also increases.

Figure 6 presents SEM images of the wear surfaces of the Ti6Al4V, N-Ti6Al4V, Ti-C:H/Ti6Al4V and Ti-C:H/N-Ti6Al4V samples following the point contact wear tests performed under a load of 10 N. The SEM image presented in Fig. 6(a) shows that the Ti6Al4V sample undergoes significant plastic deformation during sliding, resulting in the formation of deep furrows and pronounced adhesion and oxidation wear. The abrasive debris particles mainly comprise 51.99 at.% oxygen and 8.31 at.% silicon. Figure 6(b) shows that the wear surface of the N-Ti6Al4V sample experiences less plastic deformation and adhesive wear due to the increased surface hardness following the nitriding process. It also shows that the wear surface contains only relatively shallow scrape marks. Moreover, the oxygen content of the wear traces is only 8.8 at.%, while the silicon content is just 0.7 at.%. Figure 6(c) shows that the surface of the Ti-C:H/Ti6Al4V sample contains only very slight scrape marks. Moreover, the Ti-C:H coating remains virtually intact. The wear trace consists of 96.27 at.% carbon and 3.73 at.% titanium. In other words, neither oxidation nor silicon transfer from the sliding counterbody occurs during the sliding process. Figure 6(d) shows that the wear surface of the Ti-C:H/N-Ti6Al4V sample also contains only very minor scrape marks. Moreover, the wear trace once again consists only of carbon (97.04 at.%) and titanium (2.86 at.%). In other words, the Ti-C:H coating results in an extremely good tribological performance characterized by low sliding friction and high wear resistance.

3.2.2 Friction and Wear Resistance Properties in Line Contact Mode. Figure 7(a) shows the average friction coefficient values of the Ti6Al4V, N-Ti6Al4V, Ti-C:H/Ti6Al4V and Ti-C:H/N-Ti6Al4V samples when sliding against the 316L

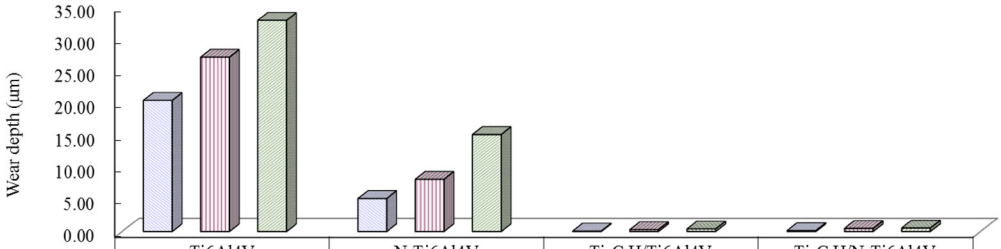

	Ti6Al4V	N-Ti6Al4V	Ti-C:H/Ti6Al4V	Ti-C:H/N-Ti6Al4V
Si3N4 10N	20.40	5.13	0.06	0.14
Standard deviation	1.442	0.362	0.004	0.010
Si3N4 20N	27.10	8.11	0.29	0.47
Standard deviation	1.530	0.458	0.016	0.026
Si3N4 30N	32.80	15.10	0.40	0.53
Standard deviation	1.391	0.640	0.016	0.022

(a)

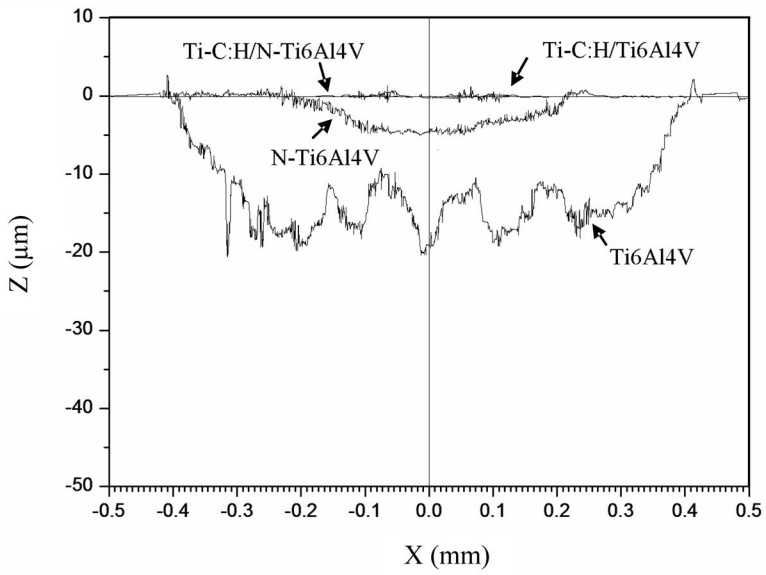

(b)

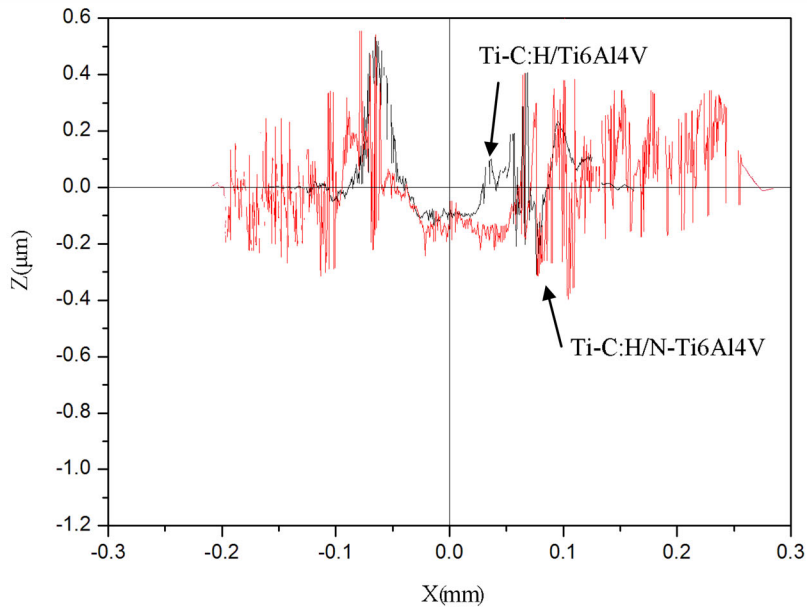

(c)

Fig. 5 Ti6Al4V samples sliding against Si_3N_4 ball: (a) histogram of average wear depth under loads of 10, 20 and 30 N, (b) wear profiles under load of 10 N and (c) magnified view of wear profiles of Ti-C:H/Ti6Al4V and Ti-C:H/N-Ti6Al4V samples under load of 10 N

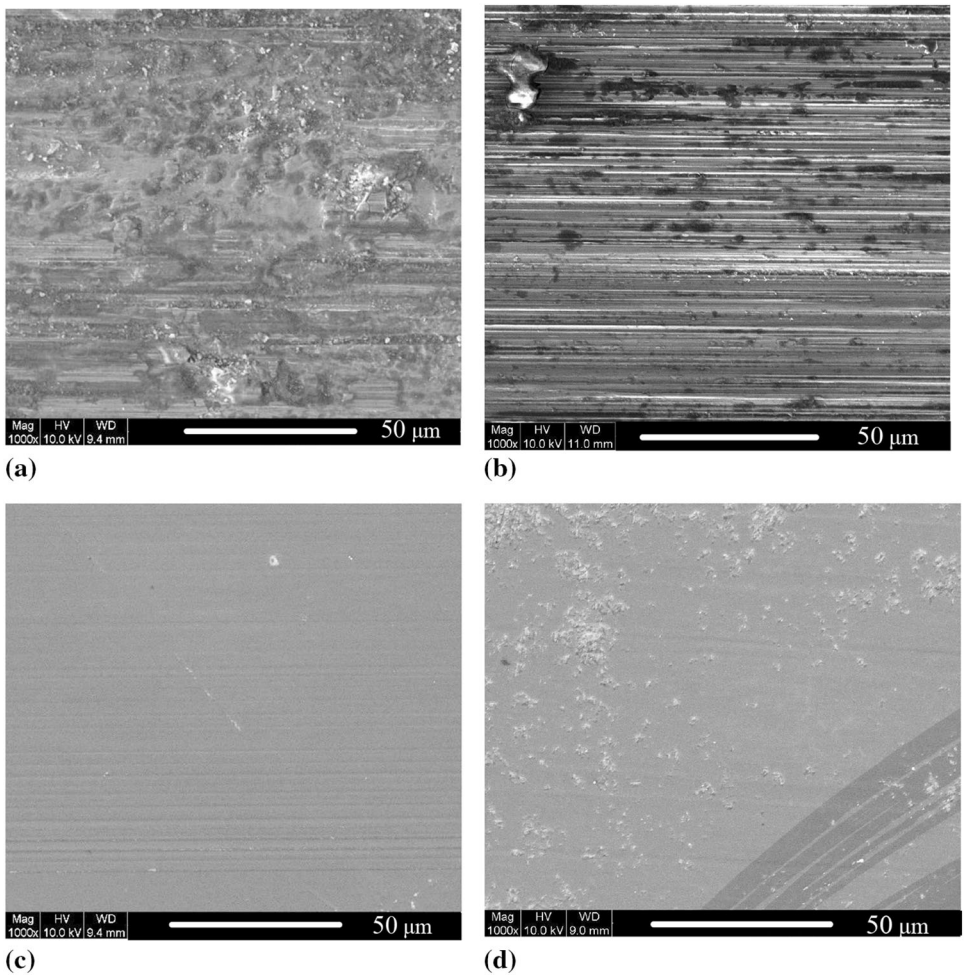

Fig. 6 SEM micrographs of wear surfaces of Ti6Al4V samples following sliding against Si_3N_4 ball under load of 10 N: (a) Ti6Al4V, (b) N-Ti6Al4V, (c) Ti-C:H/Ti6Al4V and (d) Ti-C:H/N-Ti6Al4V

stainless steel cylinder under loads of 100, 150 and 200 N. It is seen that for each sample, the friction coefficient is insensitive to the load. The Ti6Al4V sample has an average friction coefficient of about 0.56, while the nitrided sample has an average friction coefficient of approximately 0.36. The coated samples have low friction coefficients of around 0.06 (Ti-C:H/Ti6Al4V) and 0.07 (Ti-C:H/N-Ti6Al4V), respectively, i.e., around 5∼9 times lower than the uncoated samples. Figure 7(b) shows the friction coefficient trajectories of the four samples over the course of the line contact wear tests performed under a load of 100 N. The results confirm that the Ti6Al4V sample has the highest friction coefficient of the four samples (i.e., 0.575). Moreover, the friction coefficient fluctuates severely over the entire test period. The nitrided N-Ti6Al4V sample has both a lower average friction coefficient (i.e., 0.378) and a more stable friction coefficient following an initial wear-in period (approximately 122 s). For the Ti-C:H/Ti6Al4V and Ti-C:H/N-Ti6Al4V samples, the friction coefficients have average values of just 0.064 and 0.073, respectively. Moreover, both friction coefficients remain smooth and stable, with almost no fluctuations, over the entire test.

Figure 8(a) shows the average wear depths of the four samples following the line contact wear tests performed under loads of 100, 150 and 200 N. As expected, the wear depth increases with an increasing load for each sample. For example, for the Ti6Al4V sample, the wear depth increases from 20.2 to 24.7 µm as the load is increased from 100 to 200 N. The nitrided N-Ti6Al4V sample has a wear depth of just 1.78∼2.78 µm, indicating the effectiveness of the nitriding treatment in improving the wear resistance of Ti6Al4V alloy in line contact mode sliding. The wear depths of the Ti-C:H/Ti6Al4V and Ti-C:H/N-Ti6Al4V samples are further reduced to 0.14∼0.82 µm. In other words, the Ti-C:H coating provides a further improvement in the wear resistance properties of the non-nitrided and nitrided samples. Figure 8(b) shows the wear profiles of the four samples following line contact sliding under a load of 100 N. The Ti6Al4V sample has an average wear depth of 21.2 µm. By contrast, the average wear depth of the N-Ti6Al4V sample is just 1.78 µm. In other words, the nitriding treatment increases the surface hardness of the Ti6Al4V substrate and therefore inhibits plastic deformation under sliding and improves the wear resistance. The Ti-C:H/Ti6Al4V and Ti-C:H/N-Ti6Al4V samples have wear depths of 0.14 and 0.28 µm, i.e., around 151 times and 76 times, respectively, lower than that of the untreated Ti6Al4V sample (21.2 µm). Figure 8(c) presents a magnified view of the wear profiles on the N-Ti6Al4V, Ti-C:H/Ti6Al4V and Ti-C:H/N-Ti6Al4V samples. The wear depth of the Ti-C:H/N-Ti6Al4V sample is noticeably higher than that of the Ti-C:H/Ti6Al4V sample. As discussed previously in relation to Fig. 2, the Ti-C:H/Ti6Al4V

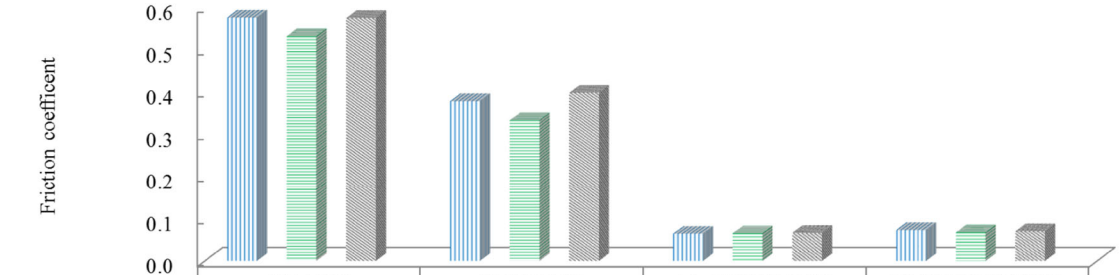

	Ti6Al4V	N-Ti6Al4V	Ti-C:H/Ti6Al4V	Ti-C:H/N-Ti6Al4V
316L 100N	0.575	0.378	0.064	0.073
standard deviation	0.041	0.027	0.005	0.005
316L 150N	0.531	0.333	0.065	0.067
standard deviation	0.038	0.024	0.005	0.005
316L 200N	0.574	0.398	0.066	0.070
standard deviation	0.041	0.028	0.005	0.005

(a)

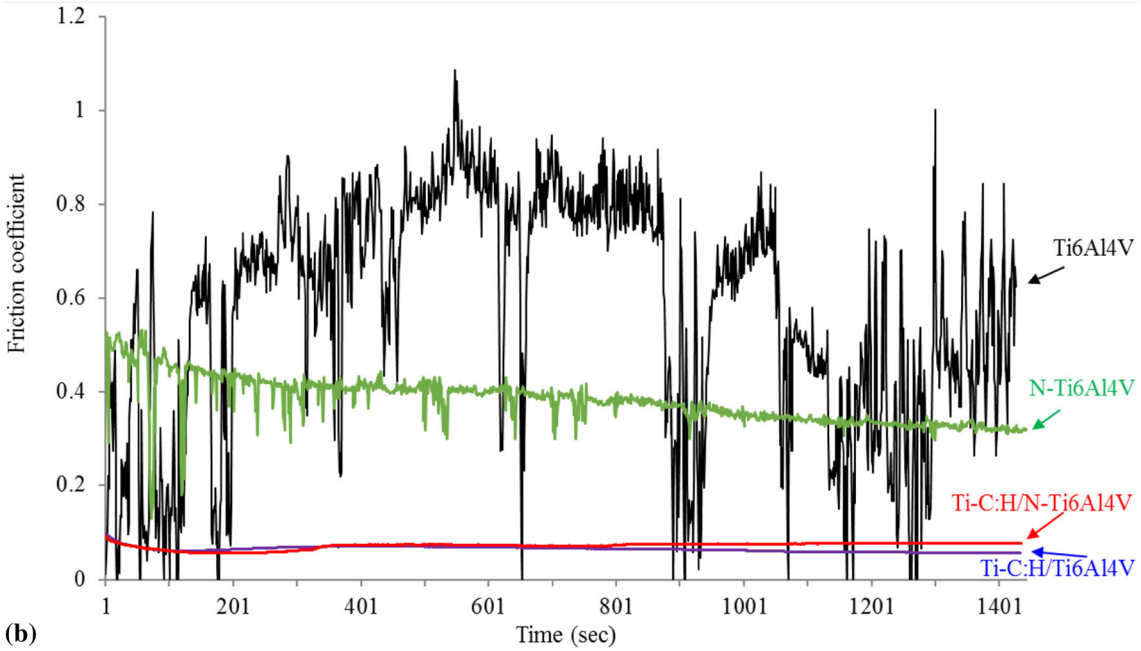

(b)

Fig. 7 Ti6Al4V samples sliding against 316L stainless steel cylinder: (a) histogram of average friction coefficient under loads of 100, 150 and 200 N and (b) friction coefficient trajectories under sliding load of 100 N

sample has a smooth and flat surface, with a roughness of just Ra = 0.03 μm. By contrast, the Ti-C:H/N-Ti6Al4V surface contains fine rough protuberances and has a roughness of Ra = 0.175 μm. The higher surface roughness induces a greater friction effect and therefore increases both the wear depth and the wear width, as shown in Fig. 8(c). Nonetheless, the Ti-C:H coating reduces the wear depth and wear rate considerably compared to that of the uncoated N-Ti6Al4V sample.

Figure 9 presents SEM micrographs of the wear surfaces of the Ti6Al4V, N-Ti6Al4V, Ti-C:H/Ti6Al4V and Ti-C:H/N-Ti6Al4V samples following sliding in the line contact mode under a load of 100 N. The micrograph in Fig. 9(a) shows that the wear surface of the untreated Ti6Al4V sample contains regions of severe plastic deformation together with flakes and small particles of abrasive debris. The debris particles have an iron content of 21.81 at.% and an oxygen content of 32.63 at.%. In other words, severe adhesion and oxidation wear occur during sliding. Figure 9(b) shows that the wear surface of the N-Ti6Al4V sample contains only shallow scrape marks. The scrape marks have an iron content of 5.11 at.% and an oxygen content of 19.19 at.%. The lower iron and oxygen contents of the nitrided specimen suggest the absence of significant adhesion or abrasive wear of the wear surface.

The wear surface of the Ti-C:H/Ti6Al4V sample also contains only slight scrape marks (see Fig. 9c). The scrape marks consist of 97.23 at.% carbon and 2.77 at.% titanium. Finally, Fig. 9(d) shows that the wear surface of the Ti-C:H/N-Ti6Al4V sample also has only a small number of minor scratches. The scratch marks contain 96.38 at.% carbon and 3.62 at.% titanium. In general, the SEM images presented in Fig. 9(c) and (d) confirm the effectiveness of the Ti-C:H coating in improving the tribological performance of Ti6Al4V

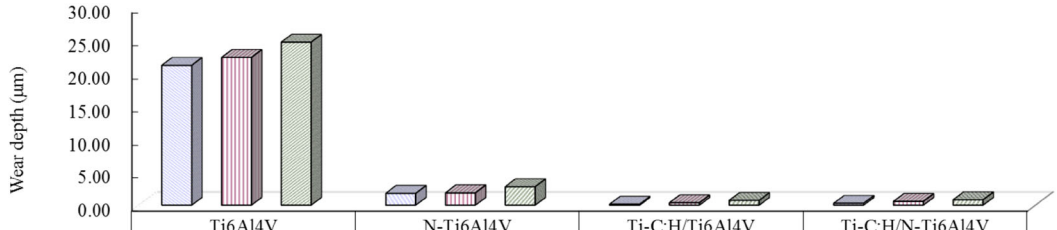

	Ti6Al4V	N-Ti6Al4V	Ti-C:H/Ti6Al4V	Ti-C:H/N-Ti6Al4V
316L 100N	21.20	1.78	0.14	0.28
Standard deviation	1.490	0.125	0.009	0.019
316L 150N	22.40	1.86	0.37	0.57
Standard deviation	1.267	0.105	0.020	0.032
316L 200N	24.70	2.78	0.72	0.82
Standard deviation	1.047	0.117	0.030	0.034

(a)

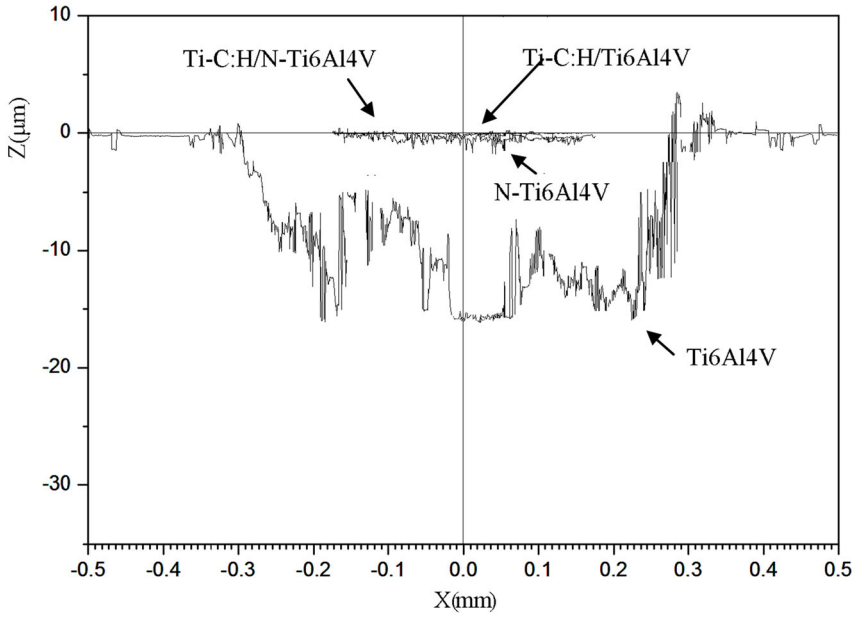

(b)

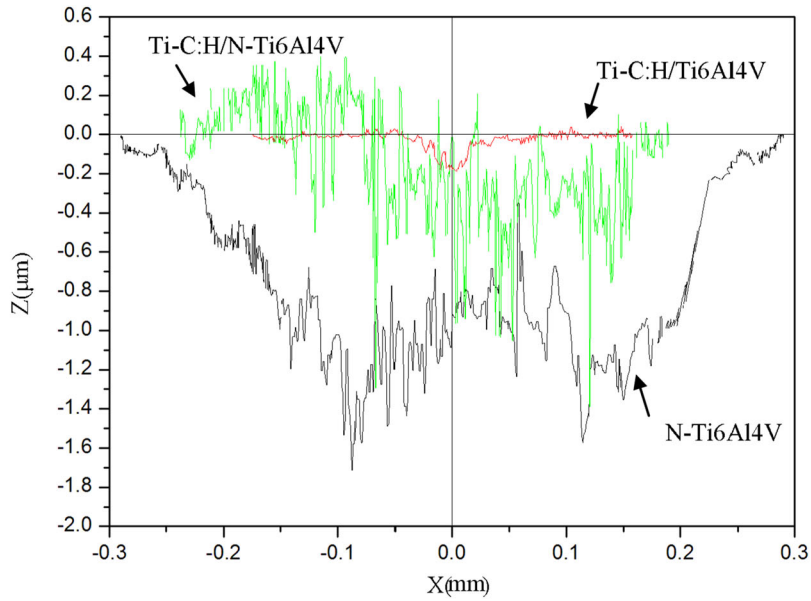

(c)

Fig. 8 Ti6Al4V samples sliding against 316L stainless steel cylinder: (a) histograms of average wear depth under loads of 100, 150 and 200 N, (b) wear profiles under load of 100 N and (c) magnified view of wear profiles of Ti-C:H/Ti6Al4V, Ti-C:H/N-Ti6Al4V and N-Ti6Al4V samples under load of 100 N

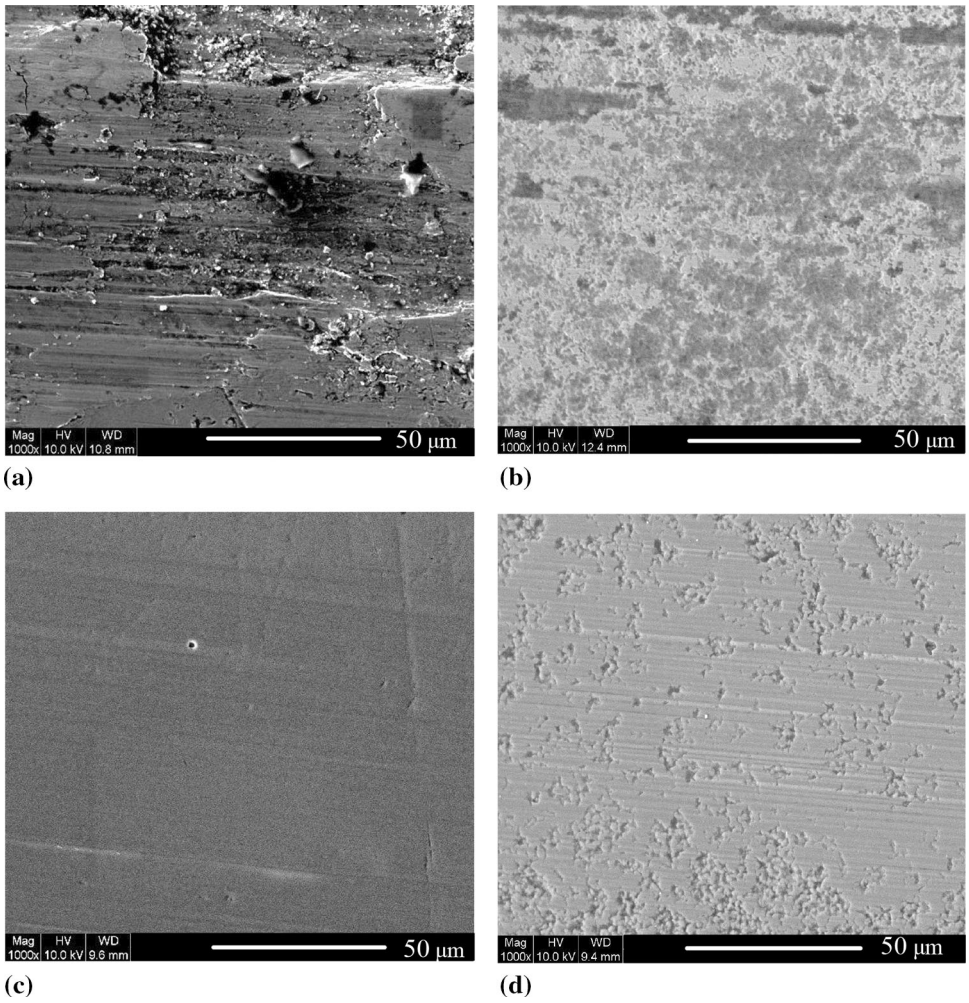

Fig. 9 SEM micrographs of wear surfaces of Ti6Al4V samples following sliding against 316L cylinder under load of 100 N: (a) Ti6Al4V, (b) N-Ti6Al4V, (c) Ti-C:H/Ti6Al4V and (d) Ti-C:H/N-Ti6Al4V

alloy in sliding against a 316L stainless cylinder in the line contact mode.

4. Summary

This study has shown that nitriding followed by the deposition of a Ti-C:H coating is beneficial in improving the tribological properties of Ti6Al4V alloy under reciprocating sliding (both point contact mode and line contact mode). In particular, the results have shown that the nitriding treatment increases the hardness of the Ti6Al4V alloy and therefore reduces both the plastic deformation and the adhesion wear. Moreover, the Ti-C:H coating yields a significant reduction in both the friction coefficient and the wear depth.

Acknowledgment

The authors gratefully acknowledge the financial support provided to this study by the Ministry of Science and Technology of Taiwan under Contract No. MOST 103-2221-E270-002.

References

1. Y.H. Zhu, K.Y. Chiu, and W.M. Tang, Polyethylene Wear and Osteolysis in Total Hip Arthroplasty, *J. Orthop. Surg.*, 2001, **9**, p 91–99
2. S. Pramanik, A.K. Agarwal, and K.N. Rail, Total Hip Joint Replacement and Materials Development, *Trends Biomater. Artif. Organs*, 2005, **19**, p 15–26
3. A. Unswotih, Recent Developments in the Tribology of Artificial Joints, *Tribol. Int.*, 1995, **28**, p 485–495
4. D. Dowson, A Comparative Study of the Performance of Metallic and Ceramic Femoral Head Components in Total Replacement Hip Joints, *Wear*, 1995, **190**, p 171–183
5. P. Bizot, L. Banallec, L. Sedel, and R. Nizard, Alumina-on-Alumina Total Hip Prostheses in Patients 40 Years of Age or Younger, *Clin. Orthop.*, 2000, **379**, p 68–76
6. P. Boyer, D. Huten, P. Loriaut, V. Lestrat, C. Jeanrot, and P. Massin, Is Alumina-on-Alumina Ceramic Bearings Total Hip Replacement the Right Choice in Patients Younger than 50 Years of Age? A 7- to 15-Year Follow-Up Study, *Orthop. Traumatol. Surg. Res.*, 2010, **96**, p 616–622
7. M. Pourbaix, Electrochemical Corrosion of Metallic Biomaterials, *Biomaterials*, 1984, **5**, p 122–134
8. LifeBridge Health Home, Conserve Plus Metal-on-Metal Hip Replacement. http://www.lifebridgehealth.org/RIAO/FDAMetalonMetalStudy.aspx

9. S.F. Harwin, FACS, Ceramic Hip Replacements & Hip Replacement Surgery. http://drharwin.com/home/
10. F.R. Marciano, L.F. Bonetti, J.F. Mangolin, N.S. Da-Silva, E.J. Corat, and V.J. Trava-Airoldi, Investigation into the Anti Bacterial Property and Bacterial Adhesion of Diamond-Like Carbon Films, *Vacuum*, 2011, **85**, p 662–666
11. F.R. Marciano, L.F. Bonetti, L.V. Santos, N.S. Da-Silva, E.J. Corat, and V.J. Trava-Airoldi, Antibacterial Activity of DLC and Ag-DLC Films Produced by PECVD Technique, *Diam. Relat. Mater.*, 2009, **18**, p 1010–1014
12. A. Almaguer-Flores, R. Olivares-Navarrete, A. Lechuga-Bernal, L.A. Ximénez-Fyvie, and S.E. Rodil, Oral Bacterial Adhesion on Amorphous Carbon Films, *Diam. Relat. Mater.*, 2009, **18**, p 1179–1185
13. Y. Ohgoe, K.K. Hirakuri, H. Saitoh, T. Nakahigashi, N. Ohtake, A. Hirata et al., Classification of DLC Films In Terms of Biological Response, *Surf. Coat. Technol.*, 2012, **207**, p 350–354
14. L. Wang, J.F. Su, and X. Nie, Corrosion and Tribological Properties and Impact Fatigue Behaviors of TiN- and DLC-Coated Stainless Steels in a Simulated Body Fluid Environment, *Surf. Coat. Technol.*, 2010, **205**, p 1599–1605
15. J. Wang and M. Liu, Study on the Tribological Properties of Hard Films Deposited on Biomedical NiTi alloy, *Mater. Chem. Phys.*, 2011, **129**, p 40–45
16. L. Randeniya, A. Bendavid, P.L. Martin, J. Cairney, A. Sullivan, S. Webster et al., Thin Film Composites of Nanocrystalline ZrO_2 and Diamond-Like Carbon: Synthesis, Structural Properties and Bone Cell Proliferation, *Acta Biomater.*, 2010, **6**, p 4154–4160
17. A.C. Martin, L. Saldana, H. Korhonen, A. Soininen, T.J. Kinnari, E.G. Barrena et al., Interactions of Human Bone Cells with Diamond-Like Carbon Polymer Hybrid Coatings, *Acta Biomater.*, 2010, **6**, p 3325–3338
18. E. Salgueiredo, M. Vila, M.A. Silva, M.A. Lopes, J.D. Santos, F.M. Costa et al., Biocompatibility Evaluation of DLC-Coated Si_3N_4 Substrates for Biomedical Applications, *Diam. Relat. Mater.*, 2008, **17**, p 878–881
19. T.L. Parker, K.L. Parker, I.R. McColl, D.M. Grant, and J.V. Wood, The Biocompatibility of Low Temperature Diamond-Like Carbon Films: A Transmission Electron Microscopy, Scanning Electron Microscopy and Cytotoxicity Study, *Diam. Relat. Mater.*, 1994, **3**, p 1120–1123
20. R. Hauert, A Review of Modified DLC Coatings for Biological Applications, *Diam. Relat. Mater.*, 2003, **12**, p 583–589
21. A.F. Yetim, A. Celik, and A. Alsaran, Improving Tribological Properties of Ti6Al4V Alloy with Duplex Surface Treatment, *Surf. Coat. Technol.*, 2010, **205**, p 320–324
22. M. Anil, S.F. Ahmed, J.W. Yi, M.W. Moon, K.R. Lee, Y.C. Kim et al., Tribological Performance of Hydrophilic Diamond-Like Carbon Coatings on Ti-6Al-4V in Biological Environment, *Diam. Relat. Mater.*, 2010, **19**, p 300–304
23. E. Arslan, Y. Totik, E.E. Demirci, and I. Efeoglu, Wear and Adhesion Resistance of Duplex Coatings Deposited on Ti6Al4V Alloy Using MAO and CFUBMS, *Surf. Coat. Technol.*, 2013, **214**, p 1–7
24. A.F. Yetima, F. Yildiz, Y. Vangolua, A. Alsarana, and A. Celika, Several Plasma Diffusion Processes for Improving Wear Properties of Ti6Al4V Alloy, *Wear*, 2009, **267**, p 2179–2185
25. S. Taktak and H. Akbulut, Dry Wear and Friction Behaviour of Plasma Nitrided Ti-6AL-4V Alloy After Explosive Shock Treatment, *Tribol. Int.*, 2007, **40**, p 423–432
26. W.H. Kao, Y.L. Su, and S.H. Yao, Improving Tribological Properties and Machining Performance of a-C Coatings by Doping with Titanium, *J. Mater. Eng. Perform.*, 2006, **15**, p 525–534
27. T. Arai, H. Fujita, and M. Watanable, Evaluation of Adhesion Strength of Thin Hard Coatings, *Thin Solid Films*, 1987, **154**, p 387–401
28. A.K. Bhattacharya and W.D. Nix, Analysis of Elastic and Plastic Deformation Associated with Indentation Testing of Thin Films on Substrates, *Int. J. Solids Struct.*, 1988, **24**, p 1287–1298